# Equilibrium and dynamics of the Ising model

Final assignment for the course of Complex Systems

*Dipartimento di Scienze Matematiche, Fisiche e Informatiche*
*Università degli Studi di Parma*

2020-2021

*Student*:
Ariel S. Boiardi *

*Professor*:
Prof. Alessandro Vezzani

## 1 Introduction

The Ising model is the paradigm of phase transitions in statistical mechanics.

The paradigmatic model of equilibrium phase transitions in statistical mechanics gets its name from the German physicist Ernst Ising who first discussed it in his 1925 thesis [4] advised by Wilhelm Lenz who was Ising's professor in Hamburg. The novelty of the model is the ability to explain magnetic phenomena as emerging from the collective behaviour of individual elementary magnets interacting locally, without the need of any other construct, such as the molecular field in Weiss' model for ferromagnetism, in opposition to which the Ising model was thought.

- Relevance of the Ising model in stat mech

*Email address: arielsurya.boiardi@studenti.unipr.it

- Loose definition
  - Magnetic properties as emerging collective behaviour
  - Model only requires local interaction
  - No need for a global field
- History
  - Lenz Ising Weiss
  - Isings solution and missed opportunities
  - KW, Onsager
- Numerical simulation
  - Parameters estimate
  - Efficient (meaning proxy) dynamic
- Contents

# 2 The Ising model

In the Ising model the magnetic material is reduced to a square lattice $\Lambda$ of size $L$ containing $N = L^2$ sites. At each site $i \in \Lambda$ is located a binary variable $s_i$ representing the magnetic dipole moment of the spin of a molecule. We assume that each spin can be either parallel or antiparallel to a fixed *easy* axis, that is $s_i = \pm 1$ for all sites.

Sites interact with each other through the magnetic fields they create, the strength of the interaction between sites $i$ and $j$ is generally denoted by $J_{ij}$; in the simplest model $J$ is constant and the interaction is limited to nearest neighbours. The energy of the system due to the interaction of the spins is $-J\sum_{\langle ij\rangle} s_i s_j$, where $\langle ij\rangle$ denotes the couples of adjacent sites on the lattice.

When $J > 0$ neighbouring spins tend to align and the material is said to be *ferromagnetic*, while for $J < 0$ the material is *anti-ferromagnetic* and neighbouring spins with the same orientation increase the energy of the system. We will generally consider $J > 0$.

If the system also interacts with an external magnetic field $h$, spin-states aligned with $h$ will have lower energy than those with the opposite orientation, the energy contribution due to the external field is therefore $-h\sum_j s_j$. Assembling the two energy terms together we get the Hamiltonian for the Ising model

$$H = -J\sum_{\langle ij\rangle} s_i s_j - h\sum_j s_j. \tag{1}$$

Configurations of the system consist of a set of $N$ variables

$$\mathbf{s} = \begin{bmatrix} s_1 & s_2 & \cdots & s_N \end{bmatrix}, \quad s_i = \pm 1 \quad \forall i = 1, \ldots, N;$$

the total number of such configurations is of course $2^N$ and the ensemble of the configurations is denoted by $\mathfrak{U}(L)$.

## 2.1 Thermodynamics of the Ising model

Having an expression of the energy of any microscopic configuration of the Ising model, we can derive macroscopic quantities relevant for the thermodynamical analysis of the system. The Helmoltz free energy per site is

$$F(\beta, h) = \frac{1}{N\beta} \log Z(\beta, h), \tag{2}$$

where $\beta = \frac{1}{k_B T}$, being $k_B$ Boltzmann's constant, is the inverse temperature, and

$$Z(\beta, h) = \sum_{\mathbf{s} \in \mathfrak{U}} e^{-\beta H(\mathbf{s})} \tag{3}$$

is the grand canonical partition function. The probability of finding the system in a configuration $\mathbf{s} \in \mathfrak{U}$ is given by the normalized Boltzmann factor

$$p(\mathbf{s}) = \frac{e^{-\beta H(\mathbf{s})}}{Z(\beta, h)}. \tag{4}$$

### 2.1.1 Macroscopic quantities from statistics of the system

The probability distribution on $\mathfrak{U}$ in (4) provides a complete statistical description of the properties of the system; furthermore standard statistical physics allows to derive all relevant macroscopic quantities from the free energy (2). A more natural description of the termodynamical properties of the system can nonetheless be given by suitable statistics.

**Magnetization** Each spin of the lattice is thought as an elementary magnet, the magnetization of a given state $\mathbf{s} \in \mathfrak{U}$ is the total dipole moment divided by the number of sites:

$$M_\Lambda(\mathbf{s}) = \frac{1}{N} \sum_{j=1}^{N} s_j; \tag{5}$$

the mean magnetization of the system is then

$$M = \langle M_\Lambda(\mathbf{s}) \rangle . \tag{6}$$

Here the angled brackets denote the thermodynamic mean in the grand canonical ensemble: given an observable $A(\mathbf{s})$

$$\langle A(\mathbf{s}) \rangle = \frac{1}{Z} \sum_{\mathbf{s} \in \mathfrak{U}} A(\mathbf{s}) e^{-\beta H(\mathbf{s})}. \tag{7}$$

The same definition for the magnetization can also be obtained as a derivative of the free energy: the total magnetization of the system is not a local property, therefore it only contributes to the energy term given by the interaction with the external magnetic field. The dependence of the free energy from the external field can therefore measure the magnetization

$$M = -\frac{\partial F(\beta, h)}{\partial h}. \tag{8}$$

The two definitions given for the magnetization prove to be equivalent:

$$\begin{aligned} -\frac{\partial F(\beta,h)}{\partial h} &= \frac{1}{N\beta Z(\beta,h)}\frac{\partial Z(\beta,h)}{\partial h} \\ &= \frac{1}{N}\frac{1}{Z(\beta,h)}\sum_{\mathbf{s}\in\mathfrak{U}}\left[e^{-\beta H(\mathbf{s})}\sum_{j=1}^{N}s_j\right] \\ &= \langle M_\Lambda\rangle\,. \end{aligned}$$

**Susceptibility** The magnetic susceptibility $\chi$ quantifies how much the material will become magnetized in response to the applied magnetic field $h$ and is therefore defined as

$$\chi = \frac{\partial M}{\partial h}. \tag{9}$$

Using the derivation of the magnetization from the free energy and some standard computations we get the well known relationship between susceptibility and fluctuations

$$\begin{aligned} \chi &= -\frac{\partial^2 F(\beta,h)}{\partial h^2} \\ &= \frac{1}{N\beta}\frac{\partial}{\partial h}\left[\frac{1}{Z}\frac{\partial Z}{\partial h}\right] \\ &= \frac{1}{N\beta}\left[-\frac{1}{Z^2}\left(\frac{\partial Z}{\partial h}\right)^2+\frac{1}{Z}\frac{\partial^2 Z}{\partial h^2}\right] \\ &= \frac{1}{N}\left[-\left\langle\sum_{j=1}^{N}s_j\right\rangle^2+\left\langle\left(\sum_{j=1}^{N}s_j\right)^2\right\rangle\right] \\ &= N\left[\left\langle M_\Lambda^2\right\rangle-\langle M_\Lambda\rangle^2\right]. \end{aligned} \tag{10}$$

### 2.1.2 Symmetry and symmetry breaking

In the expression of Ising Hamiltonian (1) for $h=0$, the value of $H$ remains invariant with respect the the transformation $\mathbf{s}\mapsto-\mathbf{s}$ which flips all spins. This fact expresses the symmetry of the system with respect to the group of transformations generated by $-\mathrm{id}$.

For each configuration $\mathbf{s}$ there is a symmetric configuration $-\mathbf{s}$, and since $H(\mathbf{s})=H(-\mathbf{s})$ the two configurations appear with the same probability. In the thermodynamic mean we therefore expect the magnetization to vanish.

**Spontaneous symmetry braking** On the other hand, in the ferromagnet different phases can coexist with opposite magnetizations: the two coexisting phases are equivalent from a physical standpoint and differ only in the prevailing direction of spins. So, even though the hamiltonian is invariant under spin flip, the thermodynamic state is not. This situation is called spontaneous symmetry breaking.

Under certain circumstance a small nonsymmetrical perturbation is sufficient to cause a violation of symmetry at the macroscopic scale. States with spins prevalently oriented in the same direction have

lower energy, but are less numerous, than those with mostly disordered spins, which prevail at high temperature. When the temperature is low enough, the energy cost of disordered states makes them not accessible; the system therefore prefers states at lower energy with non zero magnetization, as seen in fig. 1.

Which magnetization the system will take is indifferent from an energetic standpoint, but it can be fixed by letting $h \to 0^+$ or $h \to 0^-$ to get $+1$ and $-1$ magnetization respectively.

The presence of spontaneous symmmetry breaking in the two dimensional Ising model can be proved by means of a famous argument by Peierls [8]. We will follow a more experimental approach based on the simulation of the model by the Monte Carlo method.

## 2.2 In silicon experiments: simulation of the Ising model

The system naturally evolves minimizing its energy: given two states $\mathbf{s}$ and $\mathbf{s}'$ extracted at random from $\mathfrak{U}$ having an energy difference of

$$\delta H = H(\mathbf{s}') - H(\mathbf{s})$$

if $\delta H \leq 0$ the system will certainly evolve from $\mathbf{s}$ to $\mathbf{s}'$. If the energy difference is positive, the probability of the transition can be quantified by the ratio of the Boltzmann wights of the two states. All in all the transition probability is

$$W(\mathbf{s} \to \mathbf{s}') = \begin{cases} 1 & \text{if } \delta H \leq 0 \\ e^{-\beta \delta H} & \text{if } \delta H > 0. \end{cases} \tag{11}$$

Extracting successive states of the system according to this probability distribution we get a plausible evolution of the system. This extraction method was proposed by Metropolis and collaborators [7] as a correction to the Monte Carlo method for the computation of high dimensional integrals. For the Ising model the stochastic kinetics generated by the Metropolis updates (11) can be interpreted physically in terms a weak coupling of the system with the heat bath, which induces random spin flips.

### 2.2.1 Simulation algorithm

We first have to specify the size $L$ of the lattice and the boundary conditions. Then an initial configuration fo the lattice is specified.

The physical system we want to study contains a number of spins (molecules/atoms...) $N \sim 10^{23}$, which is way too big to simulate. Data obtained for numerical simulation will not completely represent the physical system, but with some tricks can be useful.

In order to extract successive states according to (11), a site $i \in \Lambda$ is extracted at random and the spin $s_i$ is considered for flipping. The energy difference $\delta H$ associated to that spin flip is computed. The evolution $s_i \mapsto -s_i$ is accepted with probability computed as (11).

Weather the considered spin is flipped or not, the configuration obtained is considered as a new configuration of the system: a rejected move is as significant as an accepted one. The physical and mathematical plausibility of this strategy is not discussed here, but the approach proves to be fruitful.

**What is time?** While the subsequent configurations generated in the simulation are a plausible representation of the "physical" Ising model, the time of the simulation has no physical meaning: the time between two subsequent extractions is arbitrary and, probably, determined by the speed of the processor crunching the numbers. After $N$ extraction we say a Monte Carlo Step (MCS) per site (or *sweep* of the lattice) has been performed. When sites are extracted at random, after one sweep some sites might have

been missed, and some considered twice, but on average all sites will be extracted the same number of times.

Since subsequent states generated by the simulation algorithm only differ by a single spin flip, their physical properties are strongly correlated. Since we want to analyse data from simulations, "measures" of the system should not be taken at every attempted spin flip, but waiting several MCSs between "measures".

**Boundary and initial conditions** Since the system we simulate needs to be much smaller that any realistic model, boundary effects are much more noticeable. The simplest solution to mitigate the disturbances coming from the boundaries is to set periodic boundary conditions: the uppermost and lowermost rows of the square lattice are regarded as neighbours, as are the leftmost and rightmost columns.

For the analysis of equilibrium properties, the initial conditions can be set more or less arbitrarily, provided that no measures are taken before the system has had enough time (MCS') to relax to equilibrium. In most simulations the initial condition has been fixed to be random (corresponding to infinite temperature). The number of sweeps needed to reach equilibrium has been determined heuristically.

## 2.3 Equilibrium phase transition

- ✓ Phase diagram
- ✓ Other critical behaviours
- • Correlation functions (Peliti)
- • Finite size scaling
- ✓ Finding the critical point by Binder cumulant

The first thing we are interested to confirm is the existence of autonomous symmetry break at $h = 0$ in the two dimensional Ising model, as this behaviour points to the existence of a phase transitions and connected critical behaviours. The plot of magnetization against temperature in fig. 1 shows indication of a phase transition occurring at a critical temperature between $k_B T \sim 1.8$ and $k_B T \sim 2.4$. The two branches of the phase diagram in fig. 1 with positive and negative magnetization are equivalent from a thermodynamic standpoint; in an infinite system (i.e. in the thermodynamic limit) there is no chance for the system to jump from one branch to the other. When the system is finite, it can fluctuate from a state of positive magnetization to a negative magnetization, even under the transition point. To avoid the problem the two branches are folded on top of each other by taking the absolute value of the magnetization [2]. Figure 2 shows the cumulated magnetization. We can better observe the transition point, but also a stronger dependence on the size of the system. smaller systems show fluctuations around the equilibrium value at higher temperatures, while bigger systems are more stable. The theoretical result of null magnetization above the critical point is only approached as the system size increases. The nonanliticity at critical temperature becomes more evident, but all curves in fig. 2 are very regular: the loss ef regularity is only possible for infinite systems, as stated by Lee and Yang's theorem [6, 5].

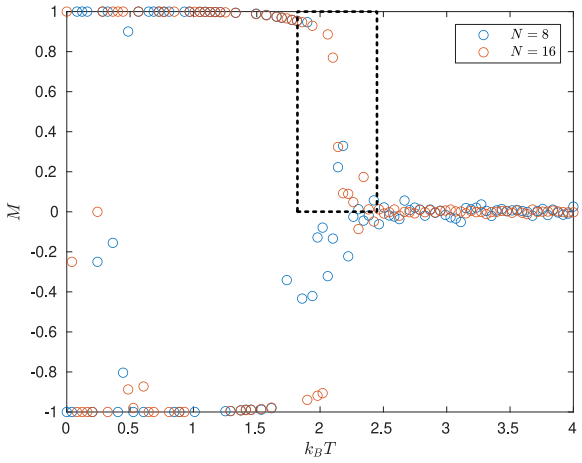


Figure 1: Magnetization measured from simulations of the system at $h = 0$. 100 temperature values uniformly sampled between 0 and 4

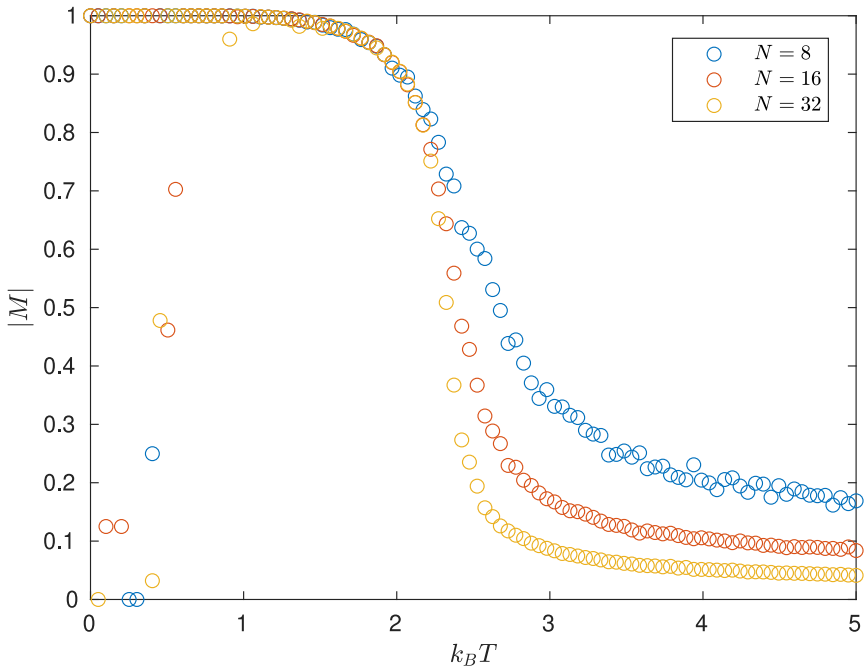


Figure 2: Cumulated magnetization: this trick makes the transition point more clear. We can also better observe the dependence on the system size.

### 2.3.1 Other critical behaviours

At the critical point the system suddenly changes its magnetic properties, therefore the susceptibility (9) has a peak singularity at the critical point that can be observed in fig. 3. Finite size effect are again evident as the susceptibility curve becomes more peaked as the system size increases.

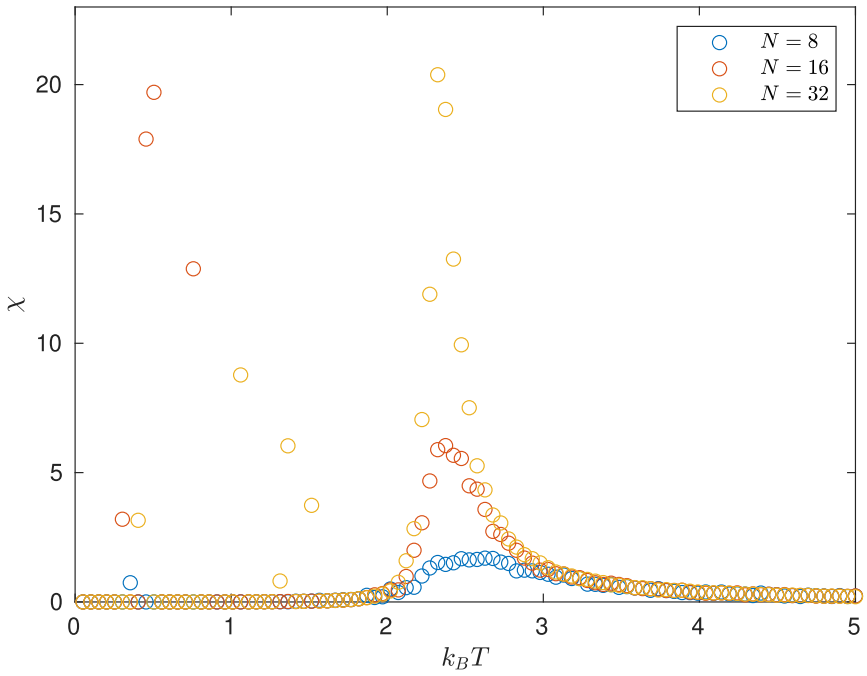


Figure 3: Magnetic susceptibility measured from simulations at $h = 0$.

**Numerical determination of the critical point** Even though the peak in the susceptibility figure can give qualitative indication of the location of the critical point, it is still difficult to estimate it with enough accuracy. The main difficulty here is that the phase transition is of the second order, i.e. the magnetization is still continuous at the critical point. Binder [1] proposed and observable, called Binder's cumulant, that presents a discontinuity at the critical point (in the thermodynamical limit)

$$U_L = \frac{1}{2}\left(3 - \frac{\langle M^4 \rangle}{\langle M^2 \rangle^2}\right). \tag{12}$$

Furthermore at the critical point, binder's cumulants computed for different finite sizes coincide, which makes it easier to uniquely determine the critical point. Unfortunately the computation of (12) is quite sensitive and very good simulation data are needed for precise result.

Figure 4 shows indeed the three curves intersecting between 2.265 and 2.285, which is consisten with the theoretical value of $T_c \approx 2.269$.

CHECK!!!

**Correlations** Even if the spin-spin interaction is strictly local, it can transmit across the lattice and create correlations between spins at distant sites. A measure fo this correlation is the *correlation function*

$$C_{ij} = \langle s_i s_j \rangle - \langle s_i \rangle \langle s_j \rangle . \tag{13}$$

The correlations between sites at distance $r$ give information about the range of at which sites interact (even if indirectly). Et the critical point

$$C_{i,i+r} \sim \frac{e^{r/\xi}}{r^{d-2+\eta}} \tag{14}$$

where the critical exponent $\xi$ describes the typical correlation distance and diverges at the critical point with power law

$$\xi \sim |T - T_c|^{-\nu} ; \tag{15}$$

$d$ is the geometric dimension of the system (2 for the square lattice) and $\eta$ is another critical exponent which we are not interested in.

# 3 Dynamic Ising model

The analysis in the previous section was about equilibrium properties of the Ising model; the simulated system was initialized with an arbitrary configuration lacking any physical significance, but "measures" of the system were only taken after the system had the time to reach equilibrium (or at least we hope so!), but the system was not observed during its evolution.

The dynamics that we observe is the sequence of configurations generated by the Monte Carlo method with Metropolis update; which we assume to be a good representation of the Ising model.

For example, in the previous analysis the initial condition was set to be random, with positive and negative spins having the same probability. The choice was arbitrary, but this state has a physical meaning: it is the equilibrium state at infinite temperature and zero magnetization. From this initial state the system is let evolve according to the Metropolis dynamic until equilibrium is reached. It has been observed that states of equilibrium for $h = 0$ and temperatures below $T_c$ have a non-zero magnetization, but of course the system does not jump from one state to the other. Some snapshots form the evolution of the system can be observed in fig. 5.

## 3.1 Quench simulation

Dynamical properties of the system can be observed when the system is cooled rapidly: the lattice is initialized at "infinite temperature" with a random configurations and the is let evolve at finite temperature $T$.

### 3.1.1 Supercritical quench

The system is cooled to a temperature $T > T_c$ above the critical point. The system does not cross the critical point, therefore the kinetics does not get slowed down. The time-displaced autocorrelation function (appendix A) plotted in fig. 7 shows that the system decorrelates in less than 100 MCS. Decorrelation in time is marginally faster than power law for configurations generated after $t_W = 10$. The linear segment in the plots of the autocorrelation function in the supercritical quench denotes a

power law decay, which on the other hand extends on a small time range right before the correlation finally drops. This behaviour can be interpreted as an effect of the finite size.

It should be noted from figs. 1 and 3 that fro finite size systems the critical temperature cannot be exactly determined, and is a bit skewed toward the right of the actual critical point, we therefore imagine that the system can show traits of the critical behaviour (power law decorrelation in time) even at supercritical temperatures. In order to observe clearly supecritical behaviours we might need to increase the temperature well above the critical point, but then the picture is not very interesting.

### 3.1.2 Critical quench

If the system is quenched at the critical point big magnetic domains for (fig. 8), and yet the temperature is still too high to allow for stable magnetized states, the isles move, resize and fluctuate. Since each update of the system is strictly local, moving these big isles becomes a slow process and decorrelation time increases compared to the supecritical case (fig. 9). We see gain in fig. 9 that for longer $t_W$ the decorrelation also becomes much slower: for longer $t_W$ bigger isles can form, and therefore the kinetics becomes slower.

Figure 8h seems to indicate a slightly magnetized state, and in fact it is. We think this is due to the dissipation at the boundary, and is therefore a finite size effect.

### 3.1.3 Subcritical quench

The system is now quenched through the phase transition at a temperature $T < T_c$ (fig. 10). At subcritical temperature configurations with aligned spins are energetically favoured; on the other hand the system evolves only locally, ad far away spins cannot influence each other. The equilibrium is achieved locally, with the formation of domains having opposite non-zero magnetizations (figs. 10b to 10e).

After these domains have formed the system is somewhat stable in the coexistence of the two magnetised phases and the dynamic becomes very slow, because, again, moving big isles of spins by local Monte Carlo updates is a slow process (figs. 10h and 10i). In this case the slow-down is not due to a critical phenomenon bu the the spontaneous breaking of symmetry in the system and the stable coexistence of the two magnetized phases.

From the analysis of the dynamic mean field we know that the relaxation to equilibrium is exponential in time, and in fact we can observe this convergence in fig. 5a. The magnetization history in fig. 10 is a bit less clear: the temperature is only slightly below the critical point, so in this case we mostly see wild fluctuations.

## 3.2 Quench on anisotropic lattices

The uniform lattice is the natural geometric structure for the Ising model, as it is a good representation of crystalline structures generally found in ferromagnetic materials. Like in a carefully engineered glass we can now introduce anisotropies in our square lattice in the form of barriers and broken links between neighbouring spins. Is it true?

The easiest way to break the crystal-like regularity of the lattice is to introduce some inert sites (represented by sites with spin 0), which do not influence the magnetic properties of the system, bu are able to break some connections between neighbouring sites.

### 3.2.1 Splitting the system

As a first experiment we introduce solid barriers at around $\frac{1}{3}$ and $\frac{2}{3}$ of the lattice in height and in width. The system is therefore split into 9 subsystems separated by walls of zero spins (inert sites). Since the updates of the lattice are local, the subsystems cannot influence each other as the walls are not "permeable".

Quenching the system at subcritical temperature (fig. 11) we observe a natural evolution of each subsystem similar to that in fig. 5. After some time the subsystems are quite independent one from each other: at the boundaries we see sharp jumps in magnetization that are only possible if the oppositely magnetized domains do not influence each other.

In the critical quench shown in fig. 12 instead we see that even for long times the pictures are not too dissimilar from the case of the critical quench without barriers (compare for example fig. 12h to fig. 8g or 8f). Big structures characteristic of the critical dynamics are still well represented and they extend well beyond the boundaries of the single subdomain.

Since it is impossible for any information to travel across the walls, we think that this is simply due to the long time persistence of long-range correlations typical of the critical dynamic. Even though the 9 subsystems evolve independently their initial conditions are correlated, as they ar all pieces of a single lattice initialized at random.

### 3.2.2 Permeable barrier

In this example the wall of null spins is a circle in the middle of the lattice, but the barrier is not solid, in order to leave an interface between the two subsystems fig. 13.

As in the previous subcritical in fig. 11) the correlation between the two subsystems become quickly very weak, and they are allowed to relax to different equilibrium configurations. Even if the barrier is permeable, and some neighbouring spins influence each other across it, the surface tension at the interface is stronger than the global energy advantage that would be achieved by equilibrating the whole system. Also notice that at $T = 0$ there is no thermal agitation, therefore the only possible evolution of the system comes from a movement of the interface between two phases.

A way to overcome this activation barrier is to introduce an external magnetic field so that the global potential, given by the configuration of the whole system, becomes stronger than the local potential due to the interface. If the magnetic field is strong enough the interior domain can quickly expand across the barrier fig. 14.

## 3.3 Nucleation

I don't know if I have the time and energy to do this...

# 4 Conclusion

In this report we reviewed the classic Ising model and some relevant thermodynamic quantities. A Monte Carlo approach based on the Metropolis update was proposed and physically motivated. An experimental approach was preferred to the rigorous mathematical and physical justification of the procedure.

The main content of the present paper is experimental: using our "in silicon" system we started reviewing the basic equilibrium properties of the Ising model, namely spontaneous symmetry breaking,

the existence of a phase transitions: the features that make this system pervasive in statistical physics. The critical point was approximated numerically using Binder's cumulant.

The study of the dynamics of the Ising model was centred on quenches.

# A Time-displaced autocorrelation function

The correlation between the values taken by one spin $s_i$ at different times $t_0$ and $t_1$ during the dynamic evolution of the Ising model is measured by the time-displaced autocorrelation $\langle s_i(t_0)s_i(t_1)\rangle$, which simply is a thermodynamical mean of the product between the two values of $s_i$ at different times. If we set a time $t_0$, we can compute the correlations of the subsequent configurations at time $t > t_0$ and taking the mean over all spins we get the autocorrelation function

$$\langle s(t_0)s(t)\rangle = \left\langle \frac{1}{N}\sum_{j=1}^{N} s_j(t_0)s_j(t) \right\rangle . \tag{16}$$

In the simulations the thermodynamic mean is obtained as a mean over many realizations of the dynamics.

# References


[1] K. Binder. "Finite size scaling analysis of ising model block distribution functions". In: *Zeitschrift für Physik B Condensed Matter* 43.2 (June 1981), pp. 119–140. DOI: 10.1007/bf01293604.

[2] K. Binder and D. W. Heermann. *Monte Carlo Simulation in Statistical Physics*. Springer Berlin Heidelberg, 2010. DOI: 10.1007/978-3-642-03163-2.

[3] G. Gallavotti. *Statistical Mechanics*. Springer Berlin Heidelberg, 1999. DOI: 10.1007/978-3-662-03952-6.

[4] E. Ising. "Beitrag zur Theorie des Ferromagnetismus". In: *Zeitschrift für Physik* 31.1 (Feb. 1925), pp. 253–258. DOI: 10.1007/bf02980577.

[5] T. D. Lee and C. N. Yang. "Statistical Theory of Equations of State and Phase Transitions. I. Theory of Condensation". In: *Physical Review* 87.3 (Aug. 1952), pp. 404–409. DOI: 10.1103/physrev.87.404.

[6] T. D. Lee and C. N. Yang. "Statistical Theory of Equations of State and Phase Transitions. II. Lattice Gas and Ising Model". In: *Physical Review* 87.3 (Aug. 1952), pp. 410–419. DOI: 10.1103/physrev.87.410.

[7] N. Metropolis et al. "Equation of State Calculations by Fast Computing Machines". In: *The Journal of Chemical Physics* 21.6 (June 1953), pp. 1087–1092. DOI: 10.1063/1.1699114.

[8] R. Peierls. "Remarks on Transition Temperatures". In: *Selected Scientific Papers of Sir Rudolf Peierls*. CO-PUBLISHED BY IMPERIAL COLLEGE PRESS AND WORLD SCIENTIFIC PUBLISHING CO., Apr. 1997, pp. 137–138. DOI: 10.1142/9789812795779_0014.

[9] L. Peliti. *Statistical Mechanics in a Nutshell*. Translated from the 2003 Italian original by Mark Epstein. Princeton University Press, Aug. 2011, pp. xviii+398. 398 pp.

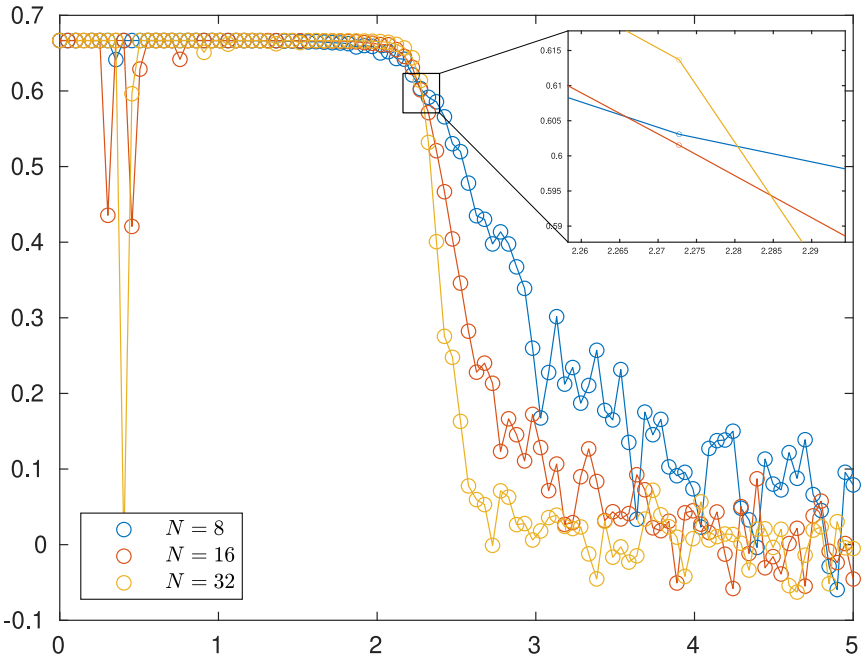


Figure 4: Binder's cumulant for three system sizes.

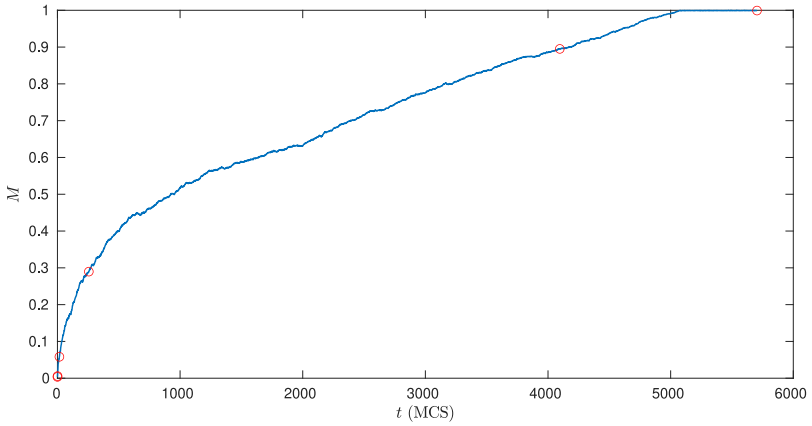


(a) Time evolution of $M$ with respect to the number of MCS. Red circles denote the points where the snapshots below were taken.

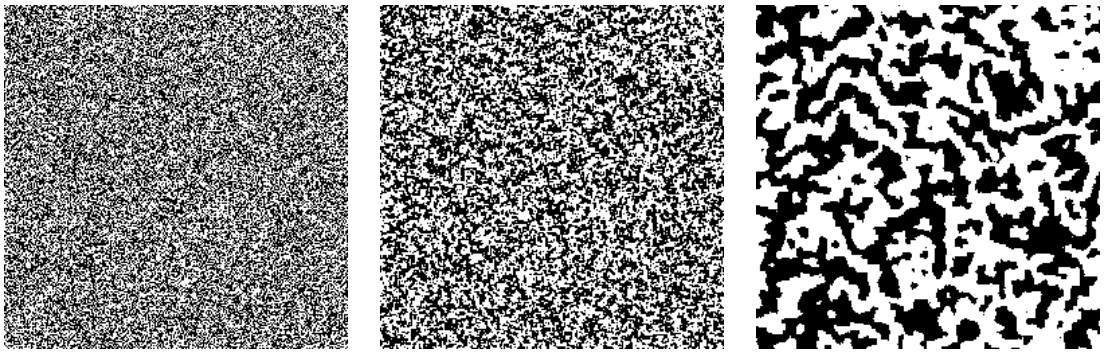

(b) $t = 0$ (c) $t = 1$ (d) $t = 16$

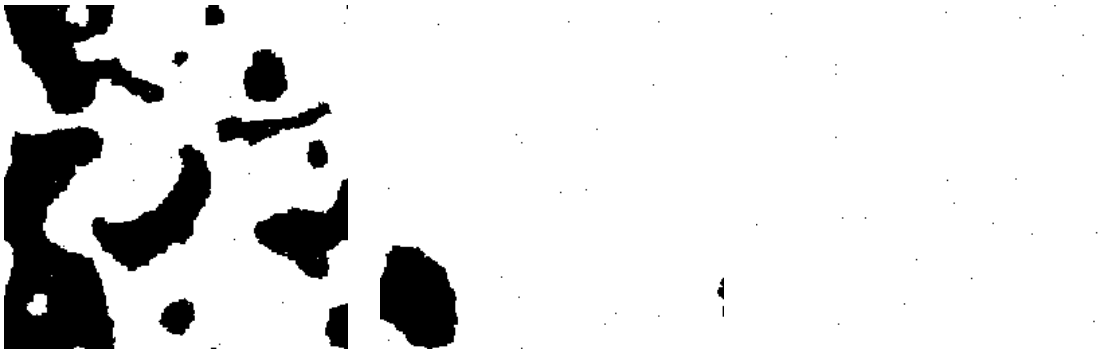

(e) $t = 256$ (f) $t = 4096$ (g) $t = 5704$

Figure 5: Evolution of the system at $k_BT = 1$, $h = 0$ from random configuration 5b to equilibrium 5g with non-zero magnetization. The value of the magnetization is also plotted against time in 5a.

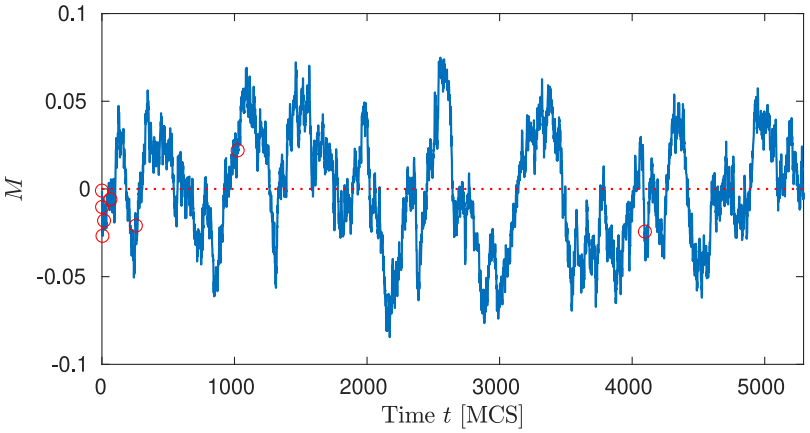


(a) Time evolution of $M$ with respect to time measured in MCS. Red circles denote the points where the snapshots below were taken. Red dotted line denoted the mean over all simulated configurations $\langle M \rangle_t \approx 1 \times 10^{-9}$.

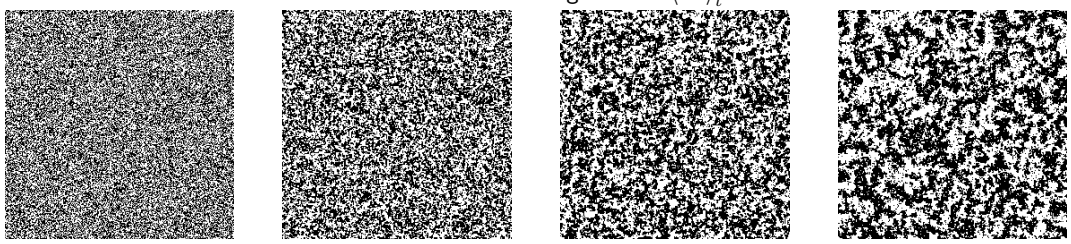

(b) $t = 0$ (c) $t = 1$ (d) $t = 4$ (e) $t = 16$

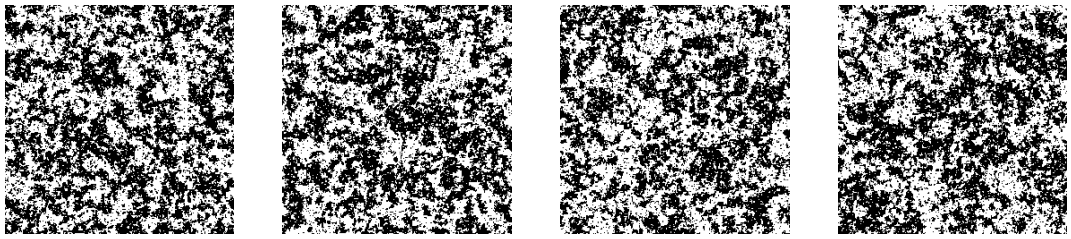

(f) $t = 64$ (g) $t = 256$ (h) $t = 1024$ (i) $t = 4096$

Figure 6: Supercritical quench at $T = 2.5$. The first four snapshots 6b-6e clearly show a progression in the evolution, characterized by the formation of bigger domains with a given magnetization. After this initial evolution the system reaches equilibrium: the following snapshots are almost not distinguishable. The existence of big magnetic domains favours big fluctuations in the magnetization 6a, which wildly oscillates about its equilibrium value.

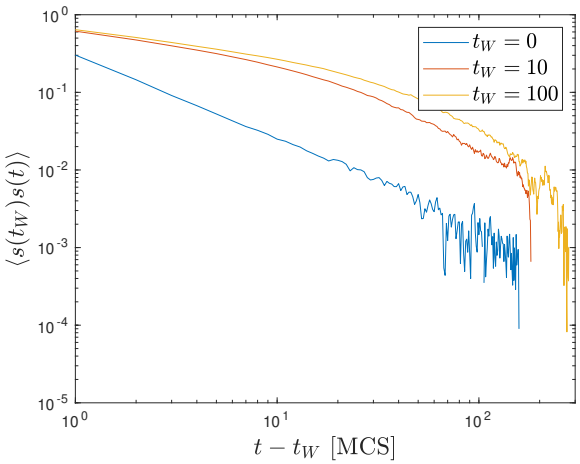


Figure 7: Time delayed autocorrelation function with respect to states at $t_W$. The random initial configuration is quenched at $T = 2.5$. System linear size $L = 128$

.

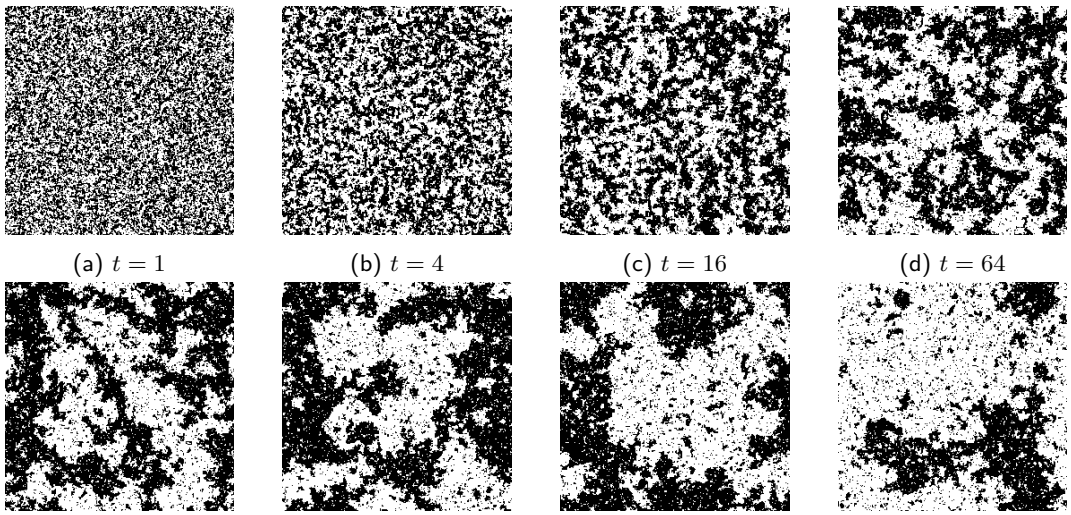

(a) $t = 1$ (b) $t = 4$ (c) $t = 16$ (d) $t = 64$

(e) $t = 256$ (f) $t = 1024$ (g) $t = 4096$ (h) $t = 16384$

Figure 8: Snapshots of the system during a critical quench.

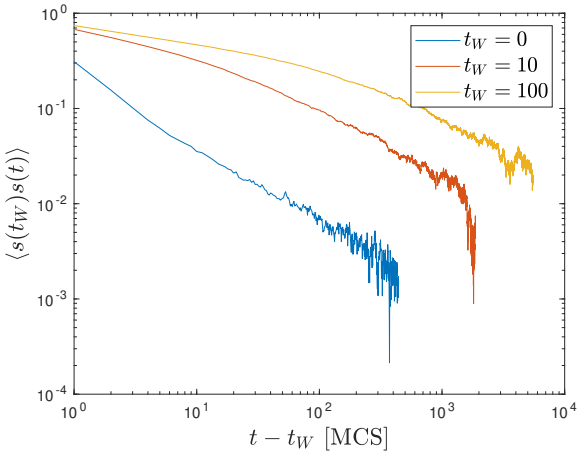


Figure 9: Time delayed autocorrelation function with respect to states at $t_W$. The random initial configuration is quenched at $T = T_C$. System linear size $L = 128$. Compared to fig. 7, we see that the time scale has increased by two orders of magnitude and the linear segments in the curves are much longer, meaning that the system decorrelates with power law in time.

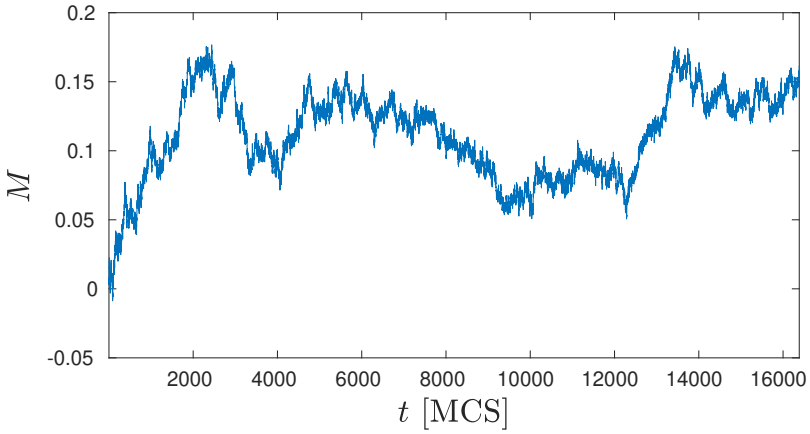


(a) Time evolution of $M$ with respect to time in MCS.

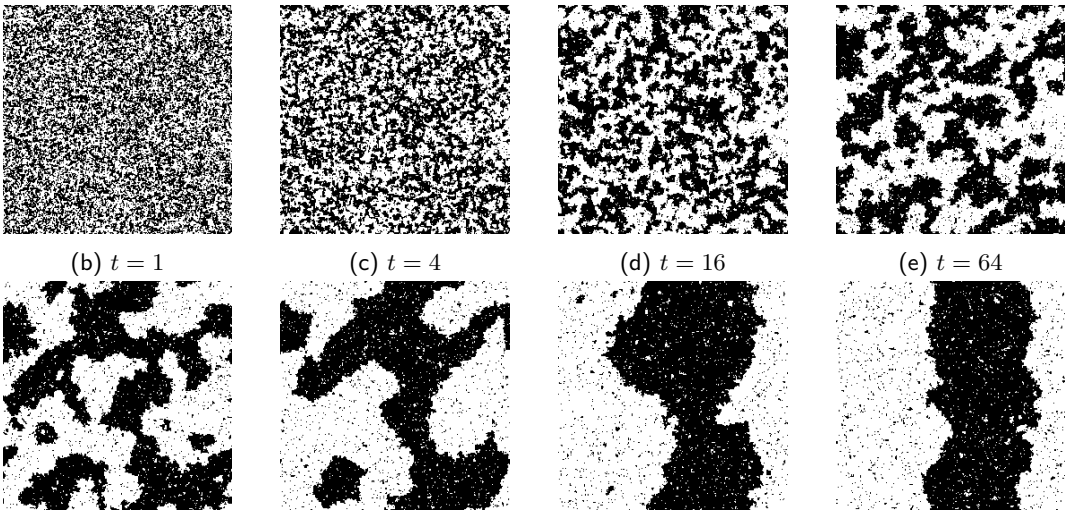

(b) $t = 1$ (c) $t = 4$ (d) $t = 16$ (e) $t = 64$

(f) $t = 256$ (g) $t = 1024$ (h) $t = 4096$ (i) $t = 16384$

Figure 10: Snapshots of the system during a subcritical quench at $T = 2$.

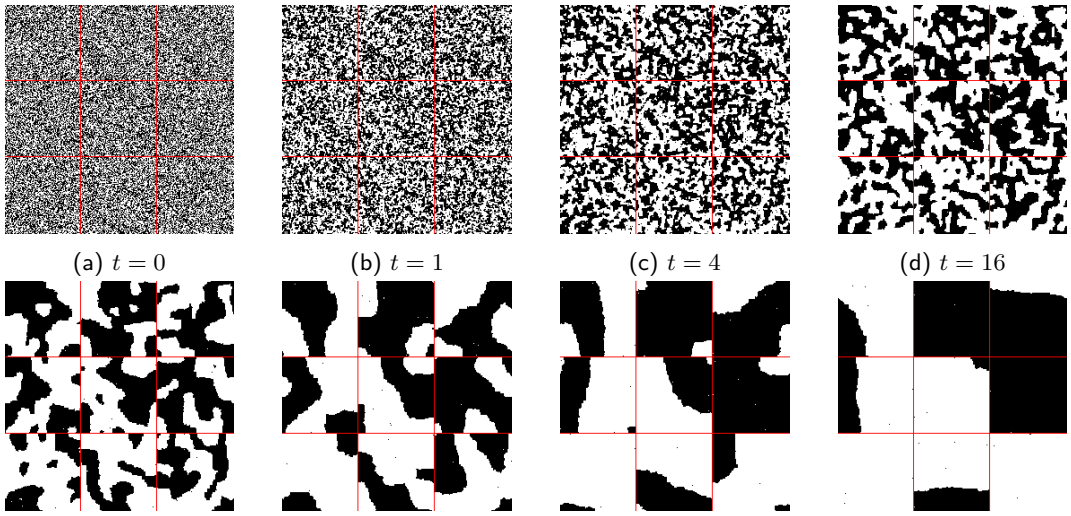

(a) $t = 0$ (b) $t = 1$ (c) $t = 4$ (d) $t = 16$

(e) $t = 64$ (f) $t = 256$ (g) $t = 1024$ (h) $t = 4096$

Figure 11: Snapshots of the subcritical quench at $T = 1$ of the system broken into subsystems discussed in section 3.2.1. Linear size of the system $L = 256$; the red walls represent the null spins.

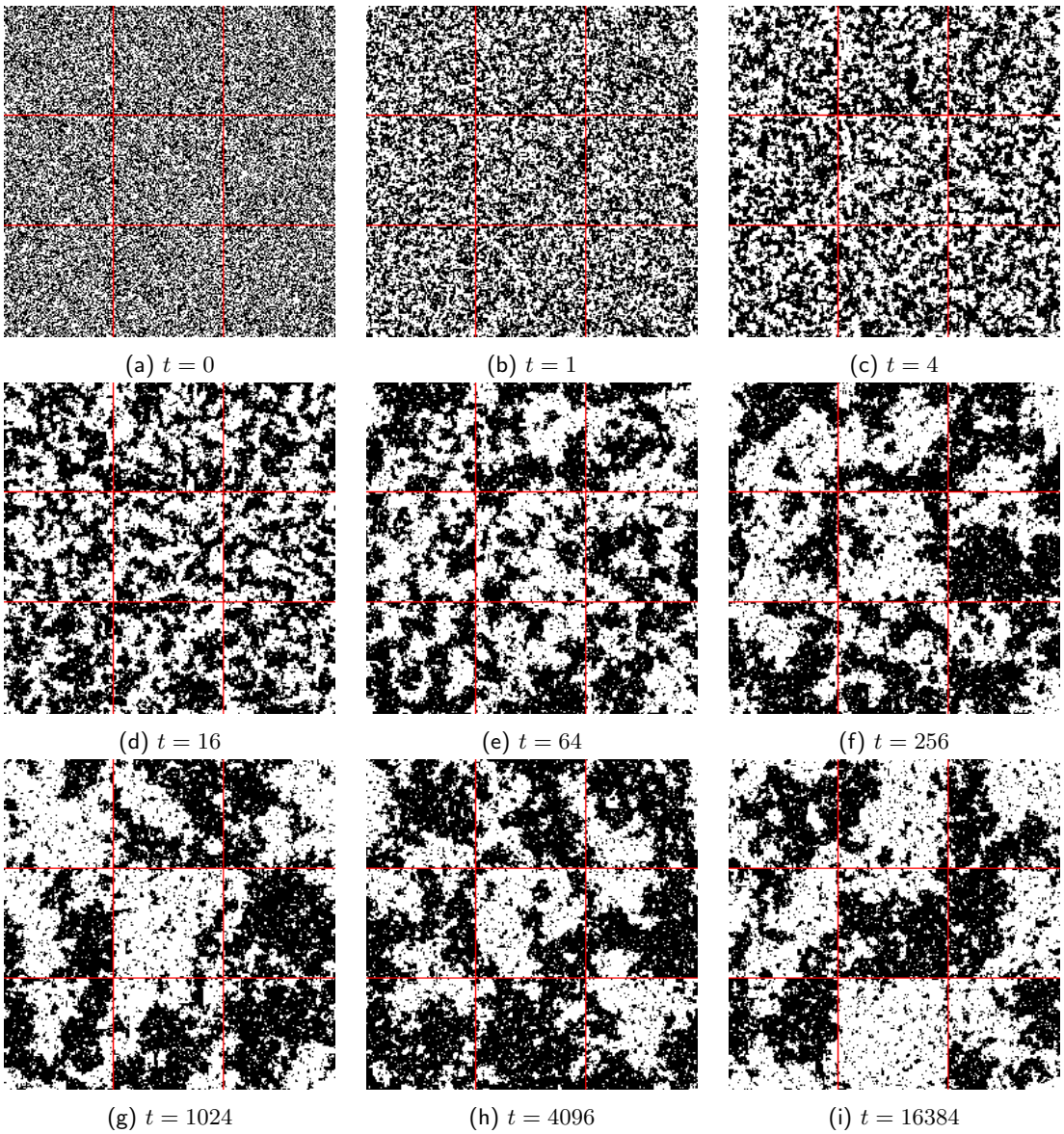

(a) $t = 0$ (b) $t = 1$ (c) $t = 4$

(d) $t = 16$ (e) $t = 64$ (f) $t = 256$

(g) $t = 1024$ (h) $t = 4096$ (i) $t = 16384$

Figure 12: Snapshots of the critical quench of the system broken into subsystems discussed in section 3.2.1. Linear size of the system $L = 256$.

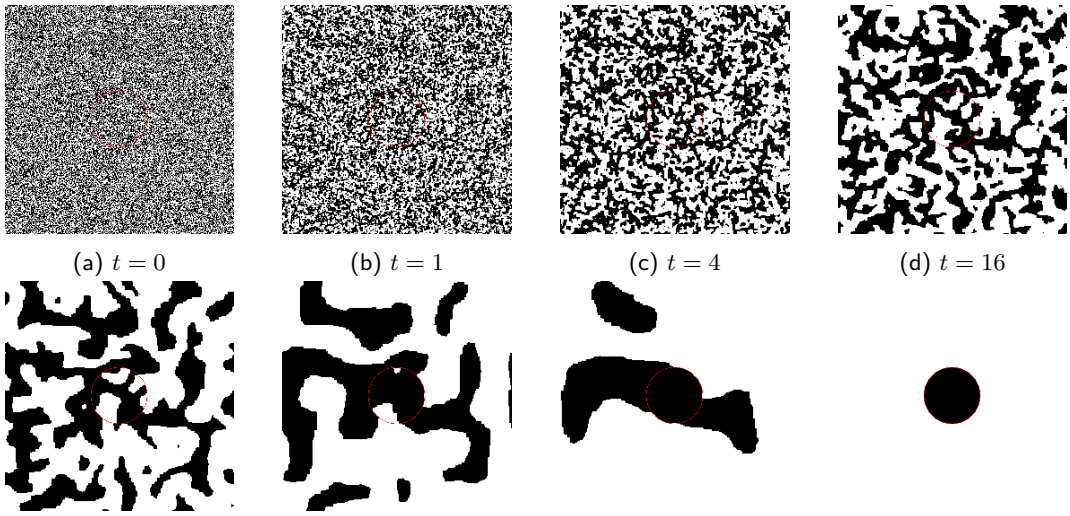

(a) $t = 0$ (b) $t = 1$ (c) $t = 4$ (d) $t = 16$

(e) $t = 64$ (f) $t = 256$ (g) $t = 1024$ (h) $t = 4096$

Figure 13: Snapshots of the subcritical quench at $T = 0$ of the system with a semipermeable circular barrier. Linear size of the system $L = 256$; the red walls represent the null spins.

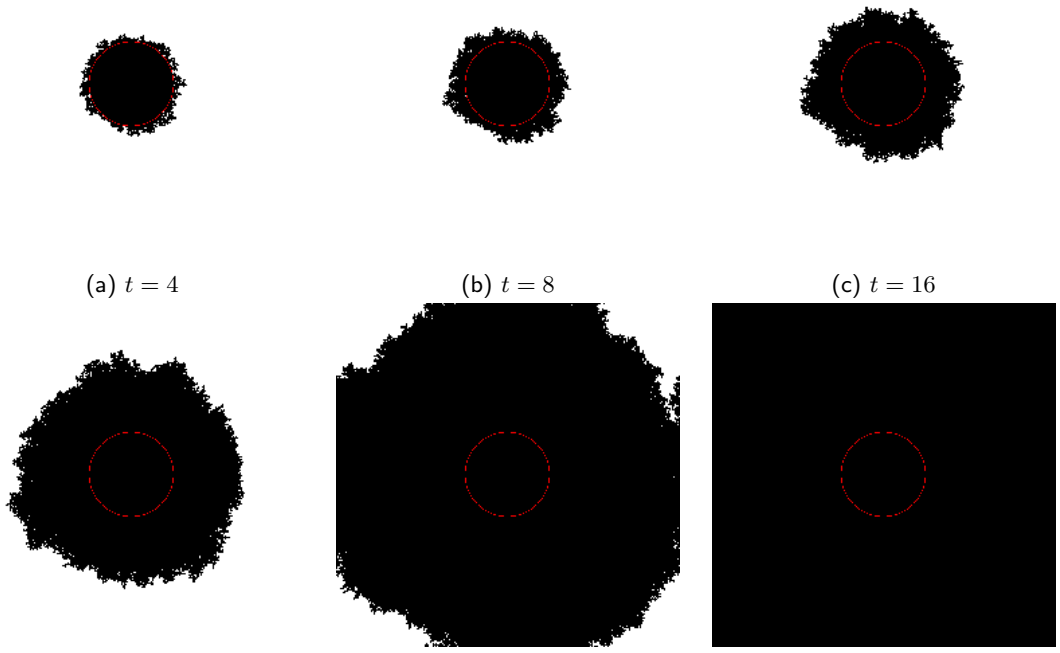

(a) $t = 4$ (b) $t = 8$ (c) $t = 16$

(d) $t = 32$ (e) $t = 64$ (f) $t = 98$

Figure 14: Evolution of the system a bit after fig. 13h with $h = 2$.